Supporting Information

de Breyne et al. 10.1073/pnas.0900153106

SI Text

Plasmids. Expression vectors for His_6-tagged WT eIF4A and eIF4B (1), pFLAG-eIF4A, His_6-tagged $eIF4G_{737–1116}$, and $eIF4G_{737–1600}$ (2), His_6-tagged $eIF4G_{737–1116}$ cysteine mutants (3), and the transcription vectors CBV3-Luc-3′UTR+A50 (4), pEV71(BrCr-TR) (5), and pIRESP1 and pIRESΔP1 (6, 7) have been described. Mutant pIRESP1 or pIRESΔP1 vectors containing PV1M $GGG_{548–550} \rightarrow AAA$ or $CCC_{453–456}/GGG_{548–550} \rightarrow UUU/AAA$ substitutions, a $GC_{461–462}$ (ΔCG) deletion, or an 8-nt (ATCGGCCG) insertion at nucleotide. 468 (+8 nt) were generated by PCR. eIF4A single-Cys substitution mutants were made to remove endogenous cysteines (Cys66Ala; Cys131Ser; Cys134Ser; Cys264Ser), followed by introduction of cysteines at positions 33, 42, 145, 167, 230, 305, 320, 351, 394 in the cysteineless eIF4A mutant.

PV1, CVB3, and EV71 plasmids were linearized with SpeI or EcoRI, ClaI, and AccI, respectively. mRNAs were transcribed in vitro by using T7 or T3 RNA polymerase.

1. Pestova TV, Hellen CUT, Shatsky IN (1996) Canonical eukaryotic initiation factors determine initiation of translation by internal ribosomal entry. *Mol Cell Biol* 16:6859–6869.
2. Lomakin IB, Hellen CU, Pestova TV (2000) Physical association of eukaryotic initiation factor 4G (eIF4G) with eIF4A strongly enhances binding of eIF4G to the internal ribosomal entry site of encephalomyocarditis virus and is required for internal initiation of translation. *Mol Cell Biol* 20:6019–6029.
3. Kolupaeva VG, Lomakin IB, Pestova TV, Hellen CU (2003) Eukaryotic initiation factors 4G and 4A mediate conformational changes downstream of the initiation codon of the encephalomyocarditis virus internal ribosomal entry site. *Mol Cell Biol* 23:687–698.
4. Dobrikova EY, Grisham RN, Kaiser C, Lin J, Gromeier M (2006) Competitive translation efficiency at the picornavirus type 1 internal ribosome entry site facilitated by viral *cis* and *trans* factors. *J Virol* 80:3310–3321.
5. Arita M, et al. (2005) Temperature-sensitive mutants of enterovirus 71 show attenuation in cynomolgus monkeys. *J Gen Virol* 86:1391–1401.
6. Pestova TV, Hellen CUT, Wimmer E (1994) A conserved AUG triplet in the 5′ nontranslated region of poliovirus can function as an initiation codon in vitro and in vivo. *Virology* 204:729–737.
7. Pestova TV, Hellen CUT, Wimmer E (1991) Translation of poliovirus RNA: Role of an essential *cis*-acting oligopyrimidine element within the 5′ nontranslated region and involvement of a cellular 57-kDa protein. *J Virol* 65:6194–6204.

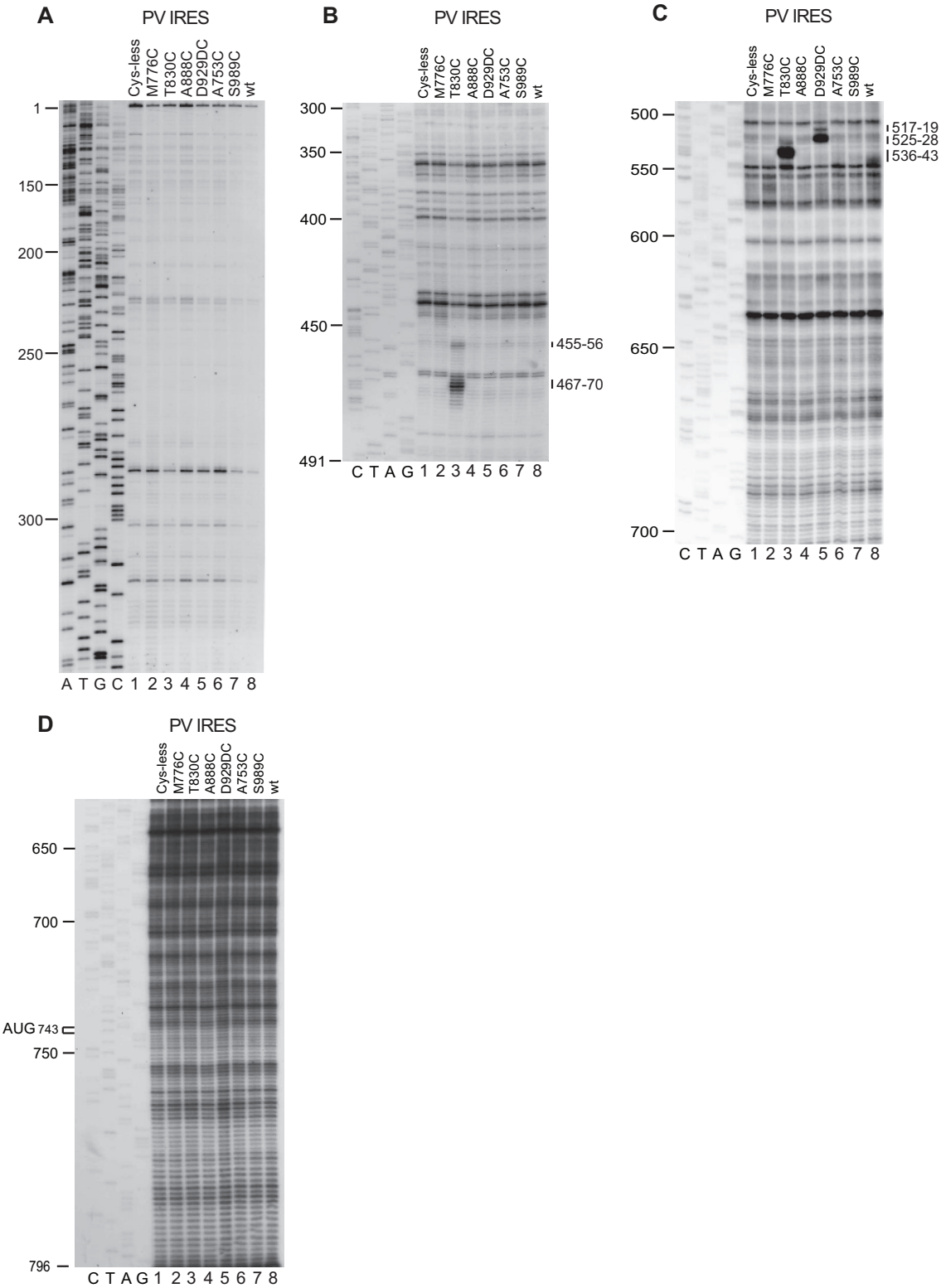

Fig. S1. Primer extension analysis of directed hydroxyl radical cleavage of PV type 1 (Mahoney) (PV1M) nucleotides 1–331 (*A*), PV1M nucleotides 300–491 (*B*), PV1M nucleotides 487–704 (*C*), and PV1M nucleotides 600–796 (*D*) from Fe(II)-tethered eIF4G mutants (as indicated) in PV1M IRES/eIF4G complexes. Primer extension analysis was done with PV1M primers listed in Table S1. Sites of hydroxyl radical cleavage are indicated to the right of *B* and *C*. Reference lanes C, T, A, and G depict viral sequences generated using the same primer; the positions of PV1M nucleotides are indicated to the left.

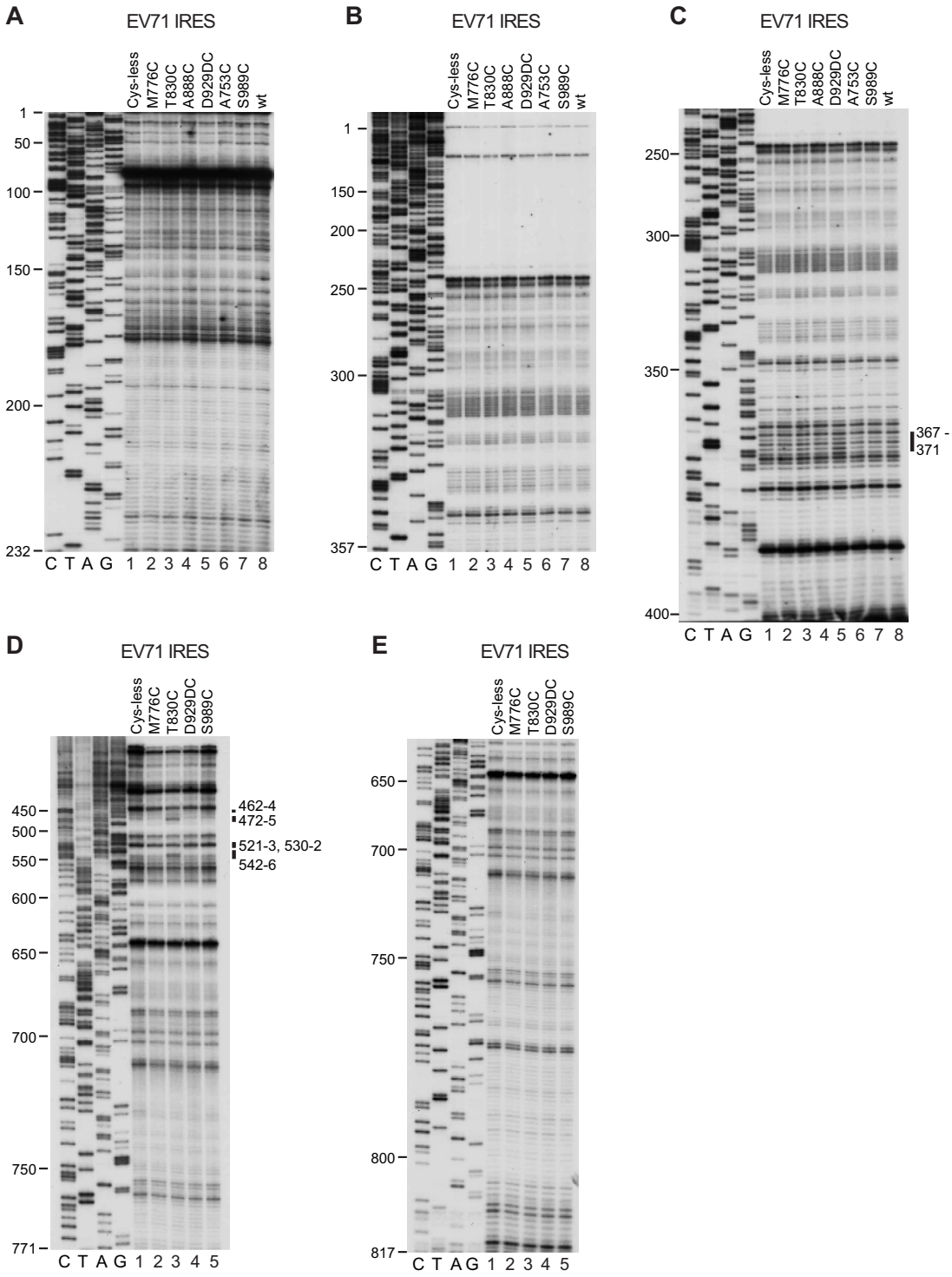

Fig. S2. Primer extension analysis of directed hydroxyl radical cleavage of EV71 nucleotides 1–232 (*A*), EV71 nucleotides 1–357 (*B*), EV71 nucleotides 208–400 (*C*), EV71 nucleotides 450–771 (*D*), and EV71 nucleotides 604–817 (*E*) from Fe(II)-tethered eIF4G mutants (as indicated) in EV71 IRES/eIF4G complexes. Primer extension analysis was done with EV71 primers listed in Table S1. Sites of hydroxyl radical cleavage are indicated to the right of *C* and *D*. Reference lanes C, T, A, and G depict viral sequences generated from the same primer; the positions of EV71 nucleotides are indicated to the left.

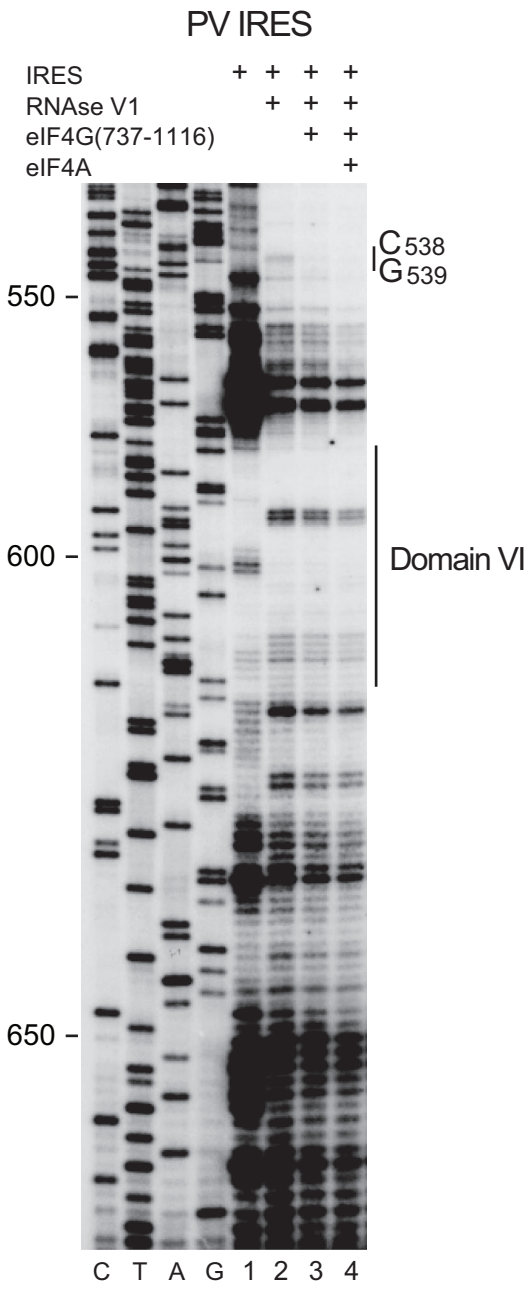

Fig. S3. Enzymatic footprinting analyses of ribonucleoprotein complexes assembled on the PV IRES. Primer extension analysis of RNase V1 cleavage of the PV1M IRES, either in mRNA alone, or complexed with eIF4GI737–1116 or eIF4GI737–1116/eIF4A, as indicated. cDNA products obtained after primer extension of untreated PV RNA are shown in lane 1. Protected residues are labeled to the right; the boundaries of IRES domain VI are also indicated and show (taking lane-to-lane variation in loading into account) that the pattern of RNase V1 cleavage in this domain and downstream is not altered by eIF4G/eIF4A. Reference lanes C, T, A, and G depict viral sequences generated from the same primer, and the positions of PV1M nucleotides at 50-nt intervals are indicated to the left.

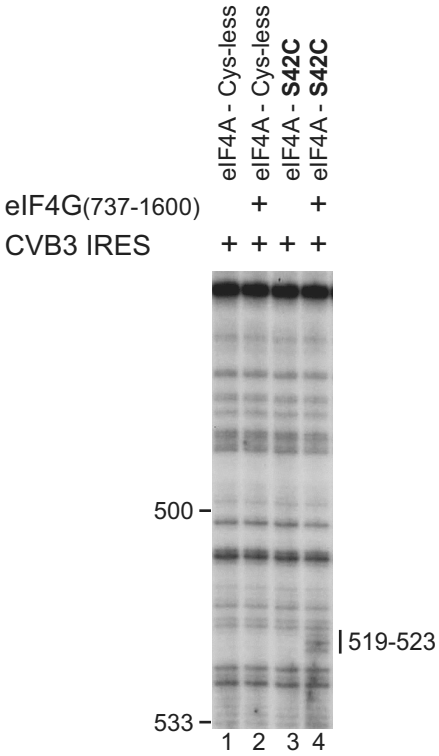

Fig. S4. Recruitment of eIF4A to the CVB3 Type 1 IRES by eIF4G. Primer extension analysis of directed hydroxyl radical cleavage of CVB3 nucleotides 475–533 from mock-derivatized cysteineless mutant eIF4A (lanes 1 and 2) and Fe(II)-tethered eIF4A (S42C) (lanes 3 and 4), in the presence or absence of eIF4G(737–1600), as indicated. Sites of hydroxyl radical cleavage are indicated to the right.

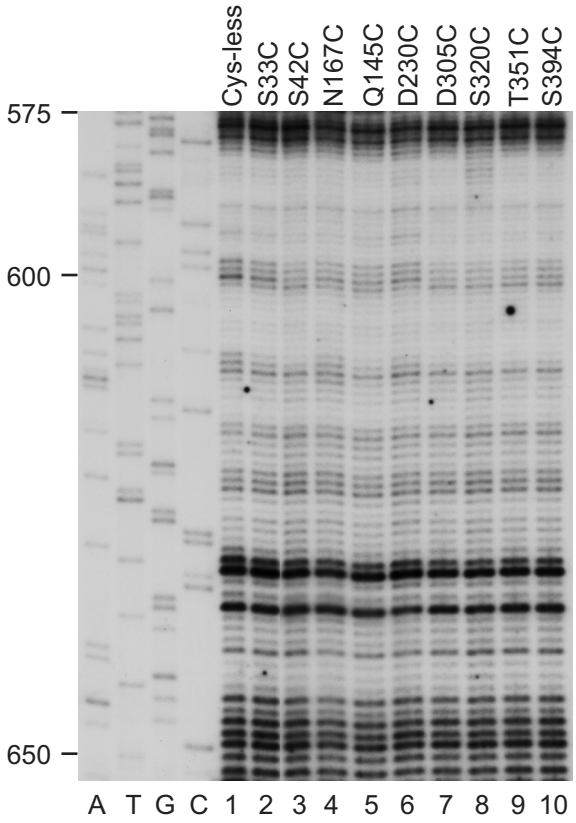

Fig. S5. Primer extension analysis of directed hydroxyl radical cleavage of PV1M nucleotides 575–652 from Fe(II)-tethered eIF4A mutants (as indicated) in PV1M IRES/eIF4G/eIF4A complexes. Lanes A, T, G, and C depict sequences generated using the same primer, and the position of PV1M nucleotides are indicated to the left.

Table S1. Oligonucleotides used for primer extension inhibition mapping of sites of directed hydroxyl radical cleavage in type 1 enterovirus IRESs

Complementary sequence	Primer sequence (5′-3′)
CVB3 nucleotides 277–259	cttccacggtgttactagg
CVB3 nucleotides 492–471	gtgtgtgctccgcagttagg
CVB3 nucleotides 612–591	acaatctctcaattgtcacc
CVB3 nucleotides 631–612	atccaatagctatatggtaa
CVB3 nucleotides 701–682	ctctttcaagctaagtggta
CVB3 nucleotides 731–711	tcaacttaacaatgaattgt
CVB3 nucleotides 870–851	cgattggctgagttggatgc
EV71 nucleotides 273–256	atggcgttactaggtttc
EV71 nucleotides 437–420	gctcaatagactcttcac
EV71 nucleotides 641–624	ggatggccaatccaatag
EV71 nucleotides 867–850	cagcagtggcagcatacg
PV1(M) nucleotides 287–268	agcgcaacgcaygcaagatt
PV1(M) nucleotides 387–368	cgttagccataggtaggccg
PV1(M) nucleotides 487–468	cacctgctccgaggttggga
PV1(M) nucleotides 587–567	cataagcagccacaataaaat
PV1(M) nucleotides 706–687	ttgtacttagagtaaacaca
PV1(M) nucleotides 833–816	taatggtggtgtaattaa